

Rhabdomyosarcomatous Differentiation in Gastrointestinal Stromal Tumors After Tyrosine Kinase Inhibitor Therapy

A Novel Form of Tumor Progression

Bernadette Liegl, MD,*† Jason L. Hornick, MD, PhD,* Cristina R. Antonescu, MD,‡
Christopher L. Corless, MD,§ and Christopher D. M. Fletcher, MD, FRCPath*

Abstract: Approximately 80% of advanced metastatic gastrointestinal stromal tumors (GISTs) respond to treatment with the tyrosine kinase inhibitor (TKI) imatinib mesylate. However, the majority of patients suffer disease progression at a median of 2 years due to drug resistance. In general, progressing GISTs retain their typical morphology. Herein, we report 5 cases of progressing metastatic GIST with heterologous rhabdomyoblastic differentiation after TKI treatment. Histologic, immunohistochemical, and mutational analyses were performed on histologically classic GISTs and components with rhabdomyoblastic differentiation. There were 3 men and 2 women (ranging from 35 to 66y of age). Three tumors were localized at presentation (2 stomach and 1 small bowel) and 2 presented with metastases. All localized primary tumors were high risk. Two tumors showed spindle cell morphology and 3 were epithelioid, including 1 with marked pleomorphism. After resection of the 3 localized primary tumors, intra-abdominal (2 patients) and liver (1 patient) metastases developed. All patients were treated with imatinib and showed partial clinical responses (4 patient) or stable disease (1 patient). Four patients subsequently progressed; 2 patients were treated with sunitinib after progression with minor responses. Four patients underwent surgical debulking. At last follow-up (range: 20 to 87 mo), 2 patients died of disease, 2 were alive with metastatic disease resistant to TKIs, and 1 was alive without evidence of disease. In all cases, rhabdomyoblastic differentiation was identified adjacent to areas with classic GIST morphology in at least 1 metastatic site; in 1 case, the primary tumor (after treatment with TKIs) showed heterologous differentiation. The rhabdomyoblastic components showed strong and diffuse positivity for desmin and expressed myogenin, whereas KIT was negative in the rhabdomyoblastic component in all cases. Primary *KIT*

mutations were detected in both the conventional GIST and rhabdomyoblastic components from all patients: *KIT* exon 11 mutations in 4 cases and a platelet-derived growth factor receptor α gene exon 18 deletion in 1 case. No secondary mutations of the type associated with TKI resistance were identified in the rhabdomyoblastic areas. This is the first report of rhabdomyoblastic differentiation occurring in GISTs that progressed on TKI therapy. It is associated with loss of *KIT* expression, but retention of the receptor tyrosine kinase mutation of the precursor GIST. The rhabdomyoblastic differentiation can represent a diagnostic pitfall. The molecular mechanisms for this form of TKI-resistant clonal evolution remain to be determined.

Key Words: GIST, rhabdomyoblastic differentiation, *KIT*, imatinib, sunitinib, tyrosine kinase

(*Am J Surg Pathol* 2008;00:000–000)

Gastrointestinal stromal tumors (GISTs) are the most common mesenchymal tumors of the gastrointestinal tract and are refractory to radiation and conventional chemotherapy. In the year 1998, Hirota and colleagues¹⁶ reported that GISTs can harbor activating mutations in the *KIT* receptor tyrosine kinase (RTK) gene and commonly express *KIT* protein by immunohistochemistry. Subsequent studies have confirmed that 85% to 90% of GISTs have activating mutations in *KIT* or the homologous RTK platelet-derived growth factor receptor α (*PDGFRA*) gene.^{13,14} The resultant constitutively activated oncoproteins serve as crucial diagnostic and therapeutic targets in GIST.^{13,14} *KIT* (CD117) is a relatively specific marker for GIST and is very helpful in the differential diagnosis of soft tissue tumors occurring in the gastrointestinal tract.^{17–19,24} Moreover, therapeutic inhibition of *KIT* and *PDGFRA* kinase activity by the tyrosine kinase inhibitor (TKI) imatinib mesylate (Gleevec, Novartis, Basel, Switzerland) has emerged as the first-line treatment for patients with metastatic or locally advanced inoperable GIST.^{6,15,26} Imatinib achieves disease control in 70% to 85% of patients with advanced GIST.^{13,26} Despite a remarkable initial response to imatinib treatment, most patients subsequently experience

From the *Department of Pathology, Brigham and Women's Hospital and Harvard Medical School, Boston, MA; †Department of Pathology, Medical University of Graz, Graz, Austria; ‡Department of Pathology, Memorial Sloan-Kettering Cancer Center, New York, NY; and §Department of Pathology, Oregon Health and Science University, Portland, OR.

Correspondence: Christopher D. M. Fletcher, MD, FRCPath, Department of Pathology, Brigham and Women's Hospital, 75 Francis Street, Boston, MA 02115 (e-mail: cfletcher@partners.org).
Copyright © 2008 by Lippincott Williams & Wilkins

disease progression due to acquired resistance. Most commonly, resistance is caused by secondary *KIT* gene mutations.^{1,5,11} Other proposed alternative resistance mechanisms include *KIT/PDGFR* genomic amplification and activation of alternative oncogenes.^{5,11} The only Food and Drug Administration-approved second-line TKI for patients with advanced GIST who have progressed on (or are intolerant of) imatinib is sunitinib malate (Sutent, Pfizer, New York, NY). Sunitinib has demonstrated efficacy, acceptable tolerability, and safety in a double-blind placebo-controlled phase 3 trial.⁷ Although progressing GISTs often acquire secondary RTK gene mutations as a mechanism for resistance to imatinib, they generally retain typical morphology after TKI treatment. Here, we report 5 cases of metastatic GIST with heterologous rhabdomyoblastic differentiation after treatment with TKI.

MATERIALS AND METHODS

GISTs with heterologous rhabdomyoblastic differentiation diagnosed between the years 2006 and 2007 were retrieved from the files of the Brigham and Women's Hospital (4 cases) and the Memorial Sloan-Kettering Cancer Center (1 case). Four micron hematoxylin and eosin-stained sections generated from formalin-fixed paraffin embedded tissue were reviewed, including initial tumor specimens and specimens received after surgery at the time of progression or at the time of autopsy. Each case was evaluated for the following: tumor cell types (spindle, epithelioid, or mixed in the conventional component; cytomorphology in rhabdomyoblastic areas), cytologic atypia, treatment effects (necrosis, hyalinosis, and hemorrhage), and mitotic rate [expressed as the number of mitotic figures per 50 high power fields (HPFs) in the most mitotically active area, using a 40 × objective and a 10 × ocular (field size 0.25 mm²)]. Risk stratification was performed according to the recent 2007 National Comprehensive Cancer Network guidelines.⁸

We performed immunohistochemical studies in all cases. The antibodies, clones, dilutions, pretreatment conditions, and sources are listed in Table 1. We used the Envision Plus detection system (Dako, Carpinteria, CA) for all antibodies. Appropriate positive and negative controls were included.

Mutational analysis was performed on areas showing classic GIST morphology and areas with rhabdomyo-

blastic differentiation. Selected paraffin-embedded tissue was deparaffinized by serial extraction with xylene and ethanol and allowed to air dry. DNA was extracted using the Qiagen minikit (no. 51304; Qiagen, Valencia, CA) in accordance with the manufacturer's recommendations. Mutational analyses were performed on the extracted genomic DNA using a combination of polymerase chain reaction amplification, denaturing high-performance liquid chromatography screening, and automated sequencing, as described previously.^{4,14} All samples were evaluated for mutations in *KIT* exons 9, 11, 13, 14, 17, and 18 and *PDGFRA* exon 12, 14, and 18.

RESULTS

Clinical Features

The clinicopathologic features and outcomes in the 5 cases studied are summarized in Table 2. A more detailed description of the patterns of tumor progression and the types and timing of treatment are provided below.

Case 1

A 53-year-old man was initially diagnosed elsewhere with a low-grade leiomyosarcoma of the small bowel. After primary resection, the patient received no adjuvant treatment and presented 2 years later with a liver metastasis. Pathology was rereviewed, and the tumor was reclassified as GIST, predominantly epithelioid type, high-risk category (15 cm; 6 mitoses/50 HPF). Treatment with imatinib 800 mg daily was initiated and the patient had stable disease for 2 years. Imatinib therapy was continued for 54 months in total. Because of progressing liver and intra-abdominal disease, the patient underwent surgical debulking. A hepatic wedge resection and resection of abdominal disease were performed. Sunitinib therapy was initiated after surgery, but the patient showed continued tumor progression and died of disease 87 months after initial diagnosis.

Case 2

A 39-year-old woman was initially diagnosed elsewhere with a metastatic spindle cell neoplasm-not otherwise specified, involving the small bowel mesentery, pancreas, and liver. Initial therapy consisted of several cycles of liposomal doxorubicin, with no apparent benefit. The pathology was rereviewed, and the tumor was

TABLE 1. Panel of Antibodies Used in This Study

Antigen	Clone	Dilution	Antigen Retrieval	Source
S-100 protein	Polyclonal	1:3000	None	Dako, Carpinteria, CA
CK (PAN-CK)	MNF116	1:700	10 min protease	Dako
c-KIT (CD117)	Polyclonal A4502	1:250	None	Dako
SMA	1A4	1:20,000	None	Sigma, St Louis, MO
Desmin	D33	1:500	None	Dako
Myogenin (MYF-4)	LO26	1:600	Heat-induced epitope retrieval	Novocastra, Burlingame, CA
CD34	QBEnd 10	1:400	None	Dako

PAN-CK indicates broad-spectrum keratin; SMA, smooth muscle actin.

TABLE 2. Clinicopathologic Features and Outcome of 5 Patients With GIST Showing Heterologous Rhabdomyoblastic Differentiation

Case	Age/Sex	Tumor	Anatomic Location	Morphology	Size (cm)	Risk assessment	Treatment	Outcome		
1	53/M	Primary	Small bowel	Epithelioid	15	High risk	None*/IM	SD on IM for 24 mo; rhabdomyoblastic differentiation after 54 mo on IM; after surgery tumor progression, resistant to both TKIs, DOD 87 mo AID		
			Liver	Epithelioid	3				Metastatic disease	
		Metastatic	Mesenteric mass	Epithelioid	15	Metastatic disease				
			Small bowel	Spindle cell	10					
	Omental mass	Rhabdomyoblastic differentiation	9							
2	39/F	Primary†	Liver biopsy	Spindle cell	6	Metastatic disease	IM	Good response/SD on IM for 10 mo; fulminant tumor progression on IM; DOD 22 mo AID; rhabdomyoblastic differentiation noted at time of autopsy		
		Metastatic disease	Omentum, peritoneum	Rhabdomyoblastic differentiation	Up to 5					
			Liver, retroperitoneum, lung, ovary, vertebra, LN	Spindle cell	Up to 20					
3	35/F	Primary	Stomach	NA	11.3	Metastatic disease	IM and SU	Good response/SD on IM for 16 mo; progression on IM (10 mo) and SU (5 mo); rhabdomyoblastic differentiation noted after 31 mo of treatment with TKIs; alive 65 mo AID with progressing disease resistant to TKIs		
		Metastatic disease	Abdomen/colonic mesentery	Pleomorphic with rhabdomyoblastic differentiation					7	
			Pelvic mass	Pleomorphic with rhabdomyoblastic differentiation						
			Ovary, peritoneal deposits, bladder	Pleomorphic with rhabdomyoblastic differentiation						Up to 3
			Mesenteric deposits	Pleomorphic with rhabdomyoblastic differentiation						Up to 3
4	57/M	Primary†	Left upper quadrant	Not evaluated	16	Not evaluated	IM and SU	Partial response/SD on IM for 10 mo; progressing on IM/SU; (1) surgery after 33 mo on TKIs (IM: 4 mo, SU: 19 mo), 1 metastasis with rhabdomyoblastic differentiation; (2) surgery 2 mo later, 9 metastases with rhabdomyoblastic differentiation under SU and gemcitabine; alive 36 mo AID, progressing disease resistant to TKIs and chemotherapy		
		Debulking surgery 1: primary tumor and adjacent progressing tumor	2 liver metastases (biopsy)	Spindle cell	Up to 9				High risk	
			Left upper quadrant mass (gastrosplenic ligament)	Rhabdomyoblastic differentiation	12.8					Primary and metastatic disease
		Debulking surgery 2: metastatic disease	9 tumors abdominal, mesenteric, and peritoneal	Rhabdomyoblastic differentiation	Up to 9				Metastatic disease	
5	66/M	Primary	Stomach	Epithelioid	20	High risk	IM	Stable metastatic disease on imatinib for 20 mo; surgical debulking, alive with no evidence of disease, on imatinib, 32 mo AID		
		Metastatic disease	Peritoneum	Rhabdomyoblastic differentiation	3.5				Metastatic disease	
			Peritoneum (multiple nodules)	Spindle cell	Up to 3.5					

*No treatment for 2 years until metastases developed.

†Presented with metastatic disease.

AID indicates after initial diagnosis; DOD, died of disease; F, female; GIST indicates gastrointestinal stromal tumor; IM, imatinib; LN, lymph node; M, male; NA, not available; SD, stable disease; SU, sunitinib; TKI, tyrosine kinase inhibitor.

reclassified as a KIT-negative GIST, spindle cell type, based on a biopsy of the liver lesion. Imatinib 400 mg daily was initiated, and the patient showed a dramatic initial response and stable disease after 10 months, clearly demonstrated on computed tomography (CT) scan. After 14 months of imatinib treatment, massive disease progression was noted on CT scan, and the patient died 22 months after initial diagnosis. At autopsy, the liver was massively enlarged (9060 g) with multiple solid white tumor nodules, up to 20 cm in size. The pancreas was adherent to a large, white, firm mesenteric tumor mass. The visceral and parietal peritoneum were studded with greater than 100 white, firm nodules ranging from 0.5 to 3 cm in size. The para-aortic retroperitoneum was involved by tumor nodules, up to 4.5 cm. Metastatic tumor was also present in the right ovary (3.5 cm), the left lung (1 cm), para-aortic lymph nodes, and the L1 vertebral body (1.8 cm).

Case 3

A 35-year-old woman presented with a 10 cm GIST in the stomach. After neoadjuvant treatment with imatinib 300 mg daily for 16 months, radical gastrectomy was performed. Imatinib therapy was discontinued 18 months after surgery due to significant fatigue. Follow-up imaging studies performed every 3 months documented abdominal disease recurrence 9 months later. Imatinib therapy was resumed with a dramatic response and near-complete resolution of a large anterior abdominal mesentery mass demonstrated by CT scan after 6 months, followed by dramatic tumor progression including pelvic disease 4 months later. Treatment with sunitinib was initiated, which showed a minor treatment effect over 5 months, after which a surgical debulking procedure was performed. The patient is alive 65 months after initial diagnosis with recurrent progressing disease, resistant to TKIs.

Case 4

A 57-year-old man presented with a 16-cm GIST in the gastrosplenic ligament and 2 liver metastases measuring 9 and 6 cm. The tumor showed a partial response to 400 mg imatinib daily, which was increased to 800 mg because of focal tumor progression on CT scan. After 14 months of imatinib treatment, the patient developed an additional 3-cm tumor nodule abutting the tumor in the gastrosplenic ligament. Sunitinib treatment was initiated, which resulted in disease control for 19 months, at which time a CT scan showed progression of the abdominal tumors and a positron emission tomography scan confirmed high metabolic activity. Surgical debulking was performed. Despite treatment with sunitinib and gemcitabine, the patient showed fulminant disease progression 2.5 months after debulking surgery. Additional surgery revealed a total of 9 tumors ranging from 0.7 to 9 cm located throughout the abdomen. The patient is alive 33 months after diagnosis with progressing disease resistant to TKIs and single agent chemotherapy.

Case 5

A 66-year-old man presented with a 20-cm primary gastric tumor, which was surgically removed. Eight months later, the patient was diagnosed with multifocal peritoneal recurrence and was started on imatinib 400 mg/d. After 14 months on imatinib therapy, clinically stable peritoneal metastases (as evaluated by CT scan, measuring 1.5 to 3.5 cm) were resected, showing an excellent treatment response microscopically. The patient resumed imatinib and is alive with no evidence of disease 33 months after initial diagnosis. However, a recent colonic biopsy showed adenocarcinoma, for which hemicolectomy is planned at the time of writing.

Microscopic Features of Pretreatment Tumor Samples

Pretreatment tumor specimens were reviewed in 4 cases (cases 1, 2, 4, and 5). Two cases (cases 2 and 4) showed typical spindle cell morphology (Fig. 1), being composed of uniform elongated cells with pale eosinophilic, fibrillary cytoplasm, ill-defined cell borders, and ovoid nuclei. The other 2 tumors (cases 1 and 5) were composed of epithelioid cells with pale eosinophilic to clear cytoplasm and round nuclei, arranged in sheets. Small areas of necrosis were seen only in case 1. Mitotic activity ranged from 6/50 HPF (case 1) to 68/50 HPF (case 5). The pretreatment specimen obtained from case 5 showed mild nuclear pleomorphism with binucleated and multinucleated forms; the other cases showed no significant atypia.

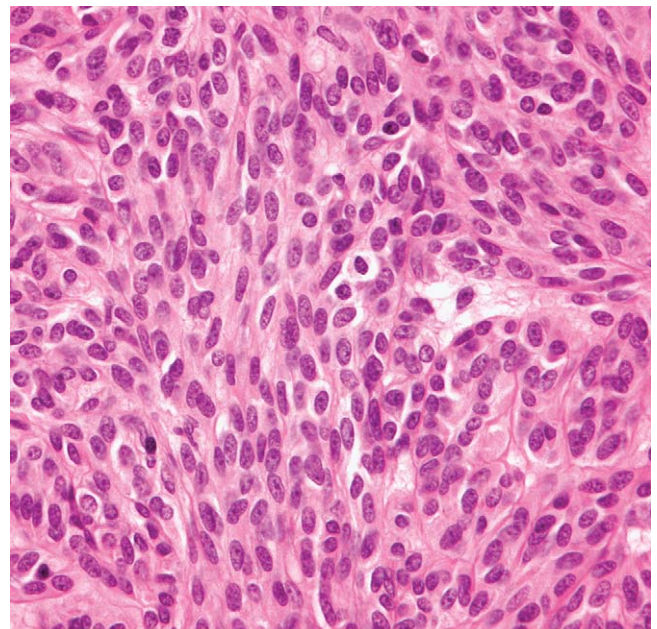


FIGURE 1. Case 2: Pretreatment tumor specimen. Typical GIST showing spindle cell morphology with pale eosinophilic, fibrillary cytoplasm, ill-defined cell borders, and uniform ovoid nuclei.

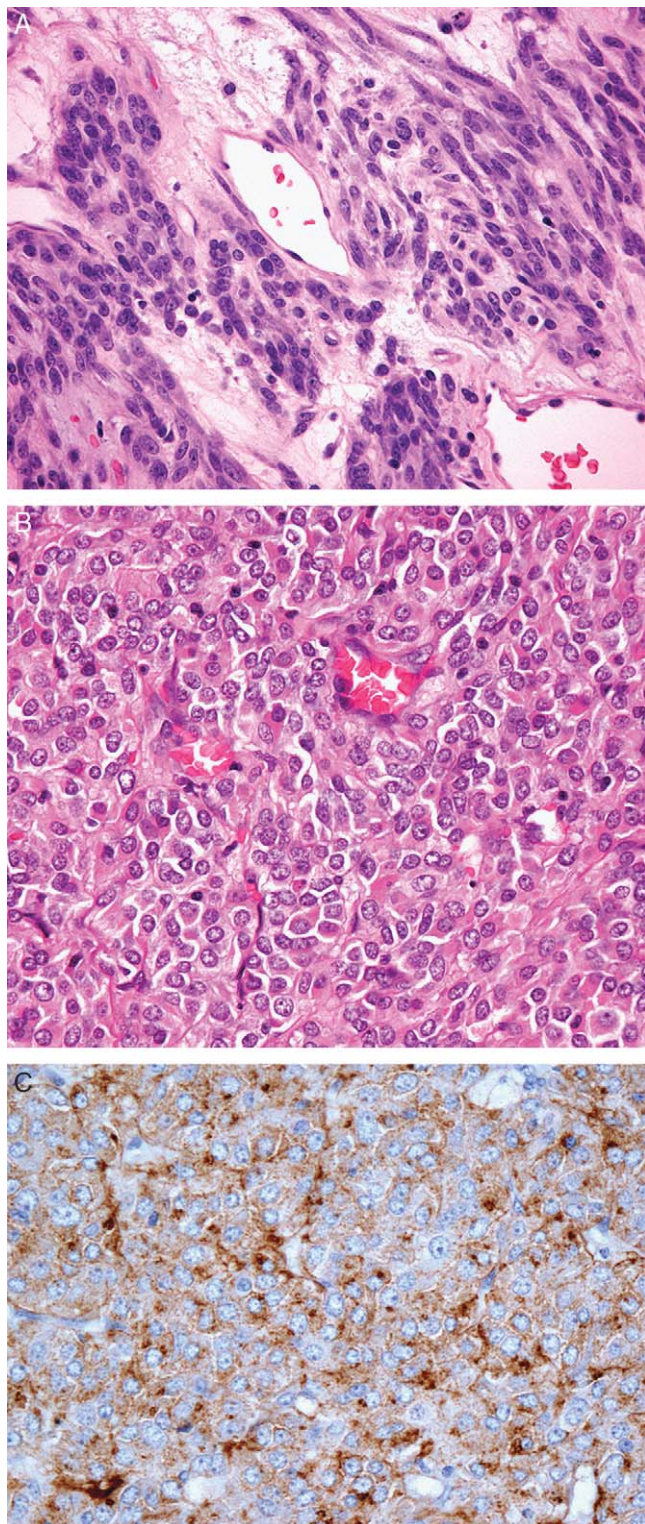


FIGURE 2. Case 1: Metastases showing spindle cell morphology in the small bowel (A) and epithelioid morphology in the liver (B), confirmed by immunopositivity for KIT (C).

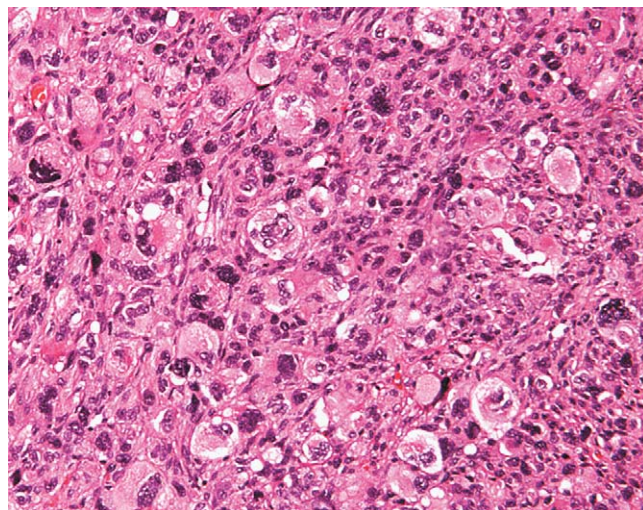


FIGURE 3. Case 3: Metastatic GIST showing marked pleomorphism, initially thought to represent treatment effect, but which proved to be rhabdomyosarcomatous differentiation.

Microscopic Features of Posttreatment Tumor Samples

In case 1, the morphologic appearances varied between different metastases [spindle and epithelioid cell type (Fig. 2)] and in case 3, tumor cells in areas of many of the metastases showed marked pleomorphism (Fig. 3), which proved to be rhabdomyoblastic in nature (see below). In case 5, the metastatic tumors showed spindle cell morphology, whereas the primary tumor in the stomach had been epithelioid.

Rhabdomyoblastic differentiation was present in metastatic lesions in all patients, and in the primary site (after neoadjuvant therapy) in 1 patient (case 4). Cases 1 and 5 showed rhabdomyoblastic differentiation in a single metastasis. In cases 2, 3, and 4, between 2 and 9 different metastases showed rhabdomyoblastic differentiation. Metastases showing rhabdomyoblastic differentiation, obtained from 4 patients (cases 1 to 4), were mainly composed of the rhabdomyoblastic component, whereas, in 1 patient (case 5), the rhabdomyoblastic focus measured only 0.7 cm within a 3.5 cm mass. In all cases, tumor areas showing rhabdomyoblastic differentiation were present next to areas with classic GIST morphology. An abrupt transition between these areas was often seen and was especially pronounced in case 3, also highlighted by the KIT immunostain (Fig. 4). The rhabdomyoblastic component was either composed of spindle cells with round to oval nuclei, focally prominent nucleoli, and amphiphilic to deeply eosinophilic cytoplasm with a bipolar or tadpole configuration resembling embryonal rhabdomyosarcoma in cases 4 and 5 (Fig. 5A), or the spindle cell component was mixed with large, polygonal tumor cells with vesicular nuclei, prominent nucleoli, and brightly eosinophilic cytoplasm resembling pleomorphic rhabdomyosarcoma in cases 1 to 3 (Fig. 5B). Occasional cytoplasmic inclusions displacing the nucleus were

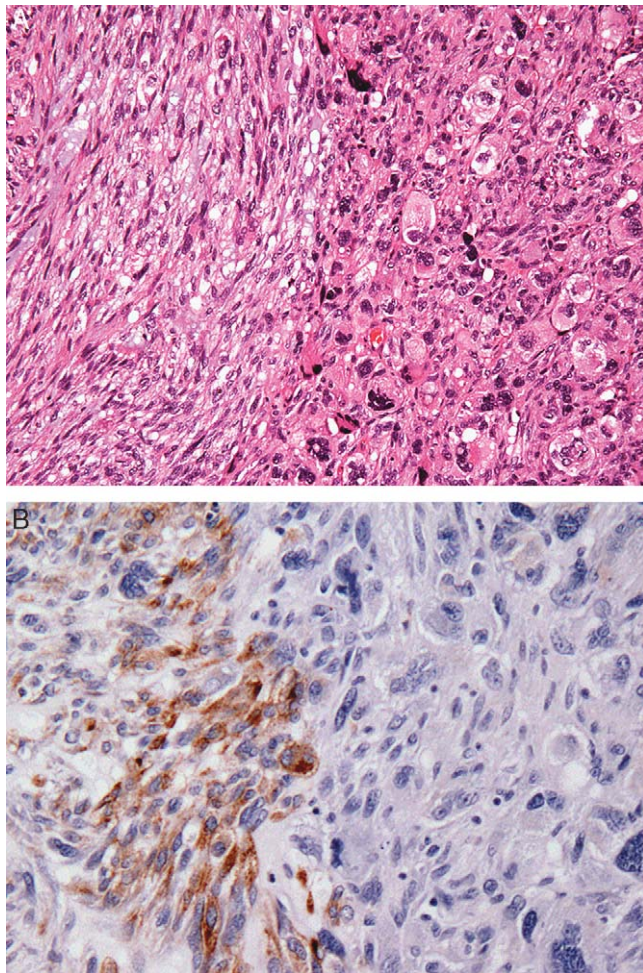


FIGURE 4. Case 3: Abrupt transition in a GIST metastasis showing spindle cell morphology to an area resembling pleomorphic rhabdomyosarcoma (A). The transition is further highlighted by loss of KIT immunopositivity in the rhabdomyoblastic component (B).

observed. Tumor specimens showed at least focal tumor necrosis, hemorrhage, and/or hyalinization in all patients. The extent of treatment response, manifest as necrosis, fibrosis, and hyalinosis, was variable and estimated as 10% to 50% in cases 1 to 4, whereas in case 5 the estimated treatment response was >95% with the exception of the viable focus with rhabdomyoblastic differentiation. Interestingly, the spindle cell component resembling classic GIST in case 4 showed pronounced hyalinization surrounding the hypercellular rhabdomyoblastic component, which showed areas of necrosis.

Immunohistochemistry

In cases 1, 3, 4, and 5, the pretreatment tumor tissue showed strong positivity with KIT (Fig. 6), whereas case 2 was KIT negative. Focal immunoreactivity with smooth muscle actin and desmin in classic-appearing GIST areas was observed in cases 1 and 2. In the posttreatment specimens, metastases showing classic GIST morphology

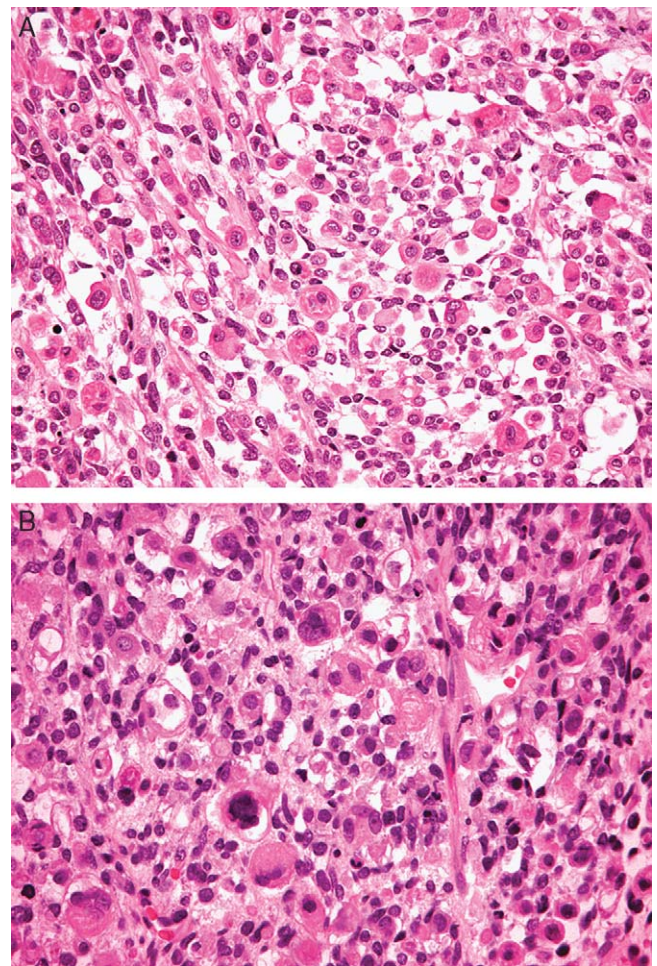


FIGURE 5. The rhabdomyoblastic component in these GIST metastases could resemble well-differentiated embryonal rhabdomyosarcoma (case 4) or more pleomorphic rhabdomyosarcoma (case 1).

expressed KIT (Fig. 2C), with the exception of case 2. The rhabdomyoblastic component present in metastases demonstrated consistently strong positivity for desmin (Fig. 7) and MYF-4 (Fig. 8) in all cases, whereas KIT was completely negative in cases 1 to 4 (Fig. 9) and only weakly expressed in case 5. CD34 was only detected in case 3. Cytokeratin (PAN-CK) was negative in all investigated cases and S-100 was focally expressed in case 4.

Mutational and Cytogenetic Analyses

The mutational findings are summarized in Table 3. In case 1, material selected from 2 blocks obtained from the omental tumor [both conventional GIST (omentum A) and the rhabdomyoblastic component (omentum B)] and material from the liver metastasis with epithelioid morphology were used for mutational analysis. In all 3 samples, a *KIT* exon 11 point mutation V559D (heterozygous) was observed; 1 sample obtained from the liver

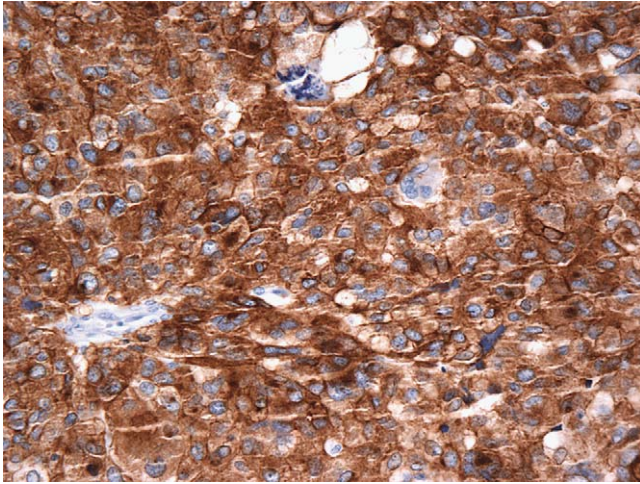


FIGURE 6. Case 1: Pretreatment epithelioid GIST showing strong KIT expression.

metastasis (epithelioid GIST) showed an additional secondary point mutation in exon 13 V654A. Mutational analysis on the omentum and liver tumor in case 2 (rhabdomyoblastic component and conventional GIST, respectively) demonstrated a *KIT* exon 11 deletion 556-574 (homozygous deletion). The tumor tissue obtained from case 3 showed an exon 11 point mutation V559D (heterozygous). Case 4 showed a *KIT* exon 11 deletion 556-574 (heterozygous deletion). Case 5 showed a *PDGFRA* exon 18 deletion and was wild type for all investigated *KIT* exons. All selected tissue samples with rhabdomyoblastic differentiation retained the primary *KIT* or *PDGFRA* mutation demonstrated in samples with classic GIST morphology. None of the samples with rhabdomyoblastic differentiation showed a secondary *KIT* resistance mutation.

Cytogenetic analysis was performed on fresh tissue obtained from patient 4 (predominantly rhabdomyoblas-

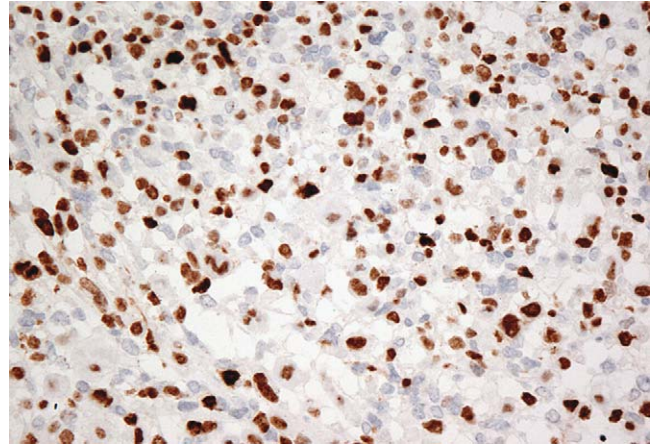


FIGURE 8. Case 4: Immunostaining shows striking nuclear MYF-4 expression in a GIST metastasis with rhabdomyoblastic differentiation.

tic component in the resected specimen). The following karyotype was obtained: 54-55, XY, +Y, +1, del (1)(p21), +6, +7, +7, +12, -14, add (16), (p13), +20, +21, +21[cp7]/46, XY [1]. Several aberrations, including 1p deletion and monosomy 14, are characteristic of GIST.

DISCUSSION

To our knowledge, this is the first report of heterologous rhabdomyoblastic differentiation developing in advanced GISTs after TKI treatment. Metastases in 5 patients treated with 1 or more TKI for 14 to 54 months showed areas reminiscent of embryonal and/or pleomorphic rhabdomyosarcoma, next to areas with classic GIST morphology. Rhabdomyoblastic differentiation was confirmed in all cases by immunohistochemical staining for desmin and MYF-4. MYF-4, the human

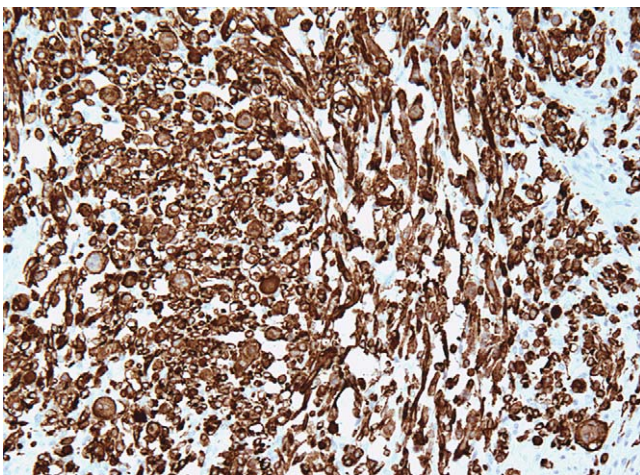


FIGURE 7. Case 4: Immunostaining demonstrates strong desmin expression in a GIST metastasis with rhabdomyoblastic differentiation.

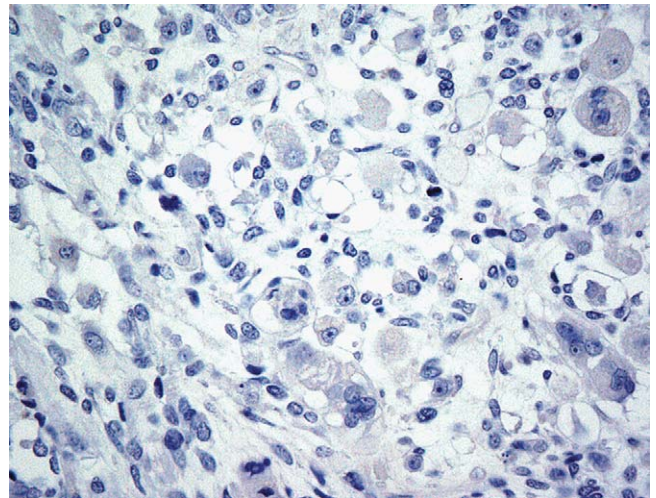


FIGURE 9. Case 1: Loss of KIT expression in the rhabdomyoblastic component of a GIST metastasis.

TABLE 3. Summary of Mutational Analysis

Case	Anatomic Location	Morphology	Mutational Analysis	
			Primary Mutation	Secondary Mutation
1	Omentum (A)	Spindle cell	<i>KIT</i> exon 11 point mutation V559D (heterozygous)	ND
	Omentum (B)	Rhabdomyoblastic differentiation	<i>KIT</i> exon 11 point mutation V559D (heterozygous)	ND
	Liver	Epithelioid	<i>KIT</i> exon 11 point mutation V559D (heterozygous)	<i>KIT</i> exon 13 V654A
2	Omentum	Rhabdomyoblastic differentiation	<i>KIT</i> exon 11 deletion 556-574 (homozygous)	ND
	Liver	Spindle cell	<i>KIT</i> exon 11 deletion 556-574 (homozygous)	ND
3	Abdomen/colonic mesentery	Pleomorphic with rhabdomyoblastic differentiation	<i>KIT</i> exon 11 point mutation V559D (heterozygous)	ND
	Mesenteric deposit	Pleomorphic with rhabdomyoblastic differentiation	<i>KIT</i> exon 11 point mutation V559D (heterozygous)	ND
4	Left upper quadrant mass (gastrosplenic ligament)	Rhabdomyoblastic differentiation	<i>KIT</i> exon 11 deletion 556-574 (heterozygous)	ND
	Left upper quadrant mass (gastrosplenic ligament)	Spindle cell	<i>KIT</i> exon 11 deletion 556-574 (heterozygous)	ND
5	Stomach	Epithelioid	<i>PDGFRA</i> exon 18 deletion, <i>KIT</i> wild-type	ND
	Peritoneum	Rhabdomyoblastic differentiation	<i>PDGFRA</i> exon 18 deletion, <i>KIT</i> wild-type	ND

ND indicates not detected; PDGFA, platelet-derived growth factor receptor α .

homolog of myogenin, accumulates in the nucleus of differentiated cells and has been shown to be a reliable marker for skeletal muscle differentiation.²⁰ Areas with classic GIST morphology expressed KIT, with the exception of case 2. Areas with heterologous rhabdomyoblastic differentiation were negative for KIT. Four cases showed a primary *KIT* exon 11 mutation and 1 case had a primary *PDGFRA* exon 18 deletion.

All patients were treated with imatinib and initially showed a treatment response according to the conventional Southwest Oncology Group/Response Evaluation Criteria in Solid Tumors.²⁵ Consistent with previous studies, the patients whose tumors harbored exon 11 mutations initially had a good clinical response to imatinib.¹³ The duration of these responses (good response/stable disease) ranged from 10 to 24 months. Interestingly, the tumor in case 2 had a hemizygous/homozygous exon 11 deletion by high-performance liquid chromatography and sequencing; this patient experienced a time interval between initial diagnosis and death of only 22 months. Metastases occurred in this case at unusual sites including lung, lymph nodes, and vertebra. Mutational analysis revealed that the exon 11 mutation in this case was a homozygous deletion. Lasota et al²¹ have reported that the presence of a homozygous exon 11 mutation is strongly associated with a malignant clinical course.

Imatinib resistance has been shown to occur, on average, after 2 years of treatment and has been demonstrated to be associated mainly with the acquisition of secondary *KIT* kinase mutations and to occur most frequently in GISTs with primary *KIT* exon 11 mutations.^{1,5,12,15} Although 4 cases in our study showed a

primary exon 11 mutation, a secondary *KIT* resistance mutation was only found in the liver metastasis from 1 case (conventional epithelioid GIST). Tissue samples showing rhabdomyoblastic differentiation retained the same primary *KIT/PDGFRA* mutation (as demonstrated in the samples with classic GIST morphology), but did not show secondary *KIT* resistance mutations.

In the absence of known resistance mechanisms, an explanation for this finding could be the clonal selection of a preexisting tumor subclone during TKI treatment. The concept of clonal selection has been proposed for the development of secondary *KIT* kinase mutations in GISTs, on the basis of findings of more than 1 secondary mutation between and within different lesions of an individual patient.^{15,22,27}

Mutational testing of samples showing heterologous rhabdomyoblastic differentiation did not shed light on specific molecular mechanisms, which might account for this unusual line of differentiation. Nevertheless, this finding, in combination with loss of KIT expression, suggests the possibility of activation of novel pathways driven by a *KIT*-independent oncogenic mechanism.

The 3 patients progressing after surgical tumor debulking and 1 patient with fulminant clinical progression were clinically resistant to treatment with TKIs. In 1 patient, who developed 9 abdominal metastases 2.5 months after initial surgery, histologic evaluation revealed rhabdomyoblastic differentiation without any treatment effect in all metastases, underscoring that TKIs failed in the setting of rhabdomyoblastic differentiation.

Other mesenchymal tumors that should be considered in the differential diagnosis of GIST with heterologous rhabdomyoblastic differentiation are dedifferentiated

liposarcoma (DDLPS) and malignant peripheral nerve sheath tumor (MPNST).^{3,9,10} Both of these tumor types may contain heterologous elements and occur in the abdomen. Approximately 10% of DDLPS and 10% to 15% of MPNST show heterologous elements,^{3,9,10} most often a rhabdomyosarcomatous component.¹⁰ With respect to DDLPS, in the absence of a well-differentiated liposarcomatous component, the differential diagnosis can be challenging, especially if the GIST is KIT negative. Sampling of fat, immunohistochemical stains for MDM2 and CDK4, and mutational analysis for *KIT/PDGFR* mutations can help to distinguish these entities.² MPNST with heterologous rhabdomyoblastic differentiation (malignant Triton tumor) is more common in patients with neurofibromatosis type 1.^{3,9} The nuclear cytomorphology, the abrupt transition between cellular and less cellular areas, the accentuation of tumor cells around blood vessels, and focal positivity for S-100 protein and/or glial fibrillary acidic protein can be diagnostically useful. However, as rhabdomyoblastic differentiation in GISTs seems limited to those tumors that have progressed on TKI therapy, so long as adequate clinical history is provided, then awareness of this phenomenon should lead to the correct diagnosis.

Although progressing GISTs usually retain typical morphology, Pauwels et al²³ previously described changes in the phenotype of GISTs under imatinib treatment. In 3 cases, a change from spindle to epithelioid or a pseudopapillary epithelioid growth pattern and loss of KIT and CD34 expression, was described.²³ Especially under these circumstances, mutational analysis is a useful diagnostic tool to confirm the correct diagnosis.

In summary, our findings demonstrate that pathologists should be aware that heterologous rhabdomyoblastic differentiation may occur in GISTs after TKI treatment and that such lesions seem to be resistant to presently available TKIs. This unusual finding (with loss of KIT expression) can represent a diagnostic pitfall. The molecular mechanisms for this form of TKI-resistant clonal evolution remain to be determined.

REFERENCES

- Antonescu CR, Besmer P, Guo T, et al. Acquired resistance to imatinib in gastrointestinal stromal tumor occurs through secondary gene mutation. *Clin Cancer Res*. 2005;11:4182–4190.
- Binh MB, Guillou L, Hostein I, et al. Dedifferentiated liposarcomas with divergent myosarcomatous differentiation developed in the internal trunk: a study of 27 cases and comparison to conventional dedifferentiated liposarcomas and leiomyosarcomas. *Am J Surg Pathol*. 2007;31:1557–1566.
- Brooks JS, Freeman M, Enterline HT. Malignant “Triton” tumors. Natural history and immunohistochemistry of nine new cases with literature review. *Cancer*. 1985;55:2543–2549.
- Corless CL, Schroeder A, Griffith D, et al. PDGFRA mutations in gastrointestinal stromal tumors: frequency, spectrum and in vitro sensitivity to imatinib. *J Clin Oncol*. 2005;23:5357–5364.
- Debiec-Rychter M, Cools J, Dumez H, et al. Mechanisms of resistance to imatinib mesylate in gastrointestinal stromal tumors and activity of the PKC412 inhibitor against imatinib-resistant mutants. *Gastroenterology*. 2005;128:270–279.
- Demetri GD, von Mehren M, Blanke CD, et al. Efficacy and safety of imatinib mesylate in advanced gastrointestinal stromal tumors. *N Engl J Med*. 2002;347:472–480.
- Demetri GD, van Oosterom AT, Garrett CR, et al. Efficacy and safety of sunitinib in patients with advanced gastrointestinal stromal tumour after failure of imatinib: a randomised controlled trial. *Lancet*. 2006;368:1329–1338.
- Demetri GD, Benjamin RS, Blanke CD, et al. NCCN Task Force report: management of patients with gastrointestinal stromal tumor (GIST)—update of the NCCN clinical practice guidelines. *J Natl Compr Cancer Netw*. 2007;5(suppl 2):S1–S29; quiz S30.
- Ducatman BS, Scheithauer BW. Malignant peripheral nerve sheath tumors with divergent differentiation. *Cancer*. 1984;54:1049–1057.
- Evans HL, Khurana KK, Kemp BL, et al. Heterologous elements in the dedifferentiated component of dedifferentiated liposarcoma. *Am J Surg Pathol*. 1994;18:1150–1157.
- Fletcher J, Corless C, Dimitrijevic S, et al. Mechanisms of resistance to imatinib mesylate (IM) in advanced gastrointestinal stromal tumors (GIST). *Proc Am Soc Clin Oncol*. 2003;22:3275–3277.
- Heinrich MC, Corless CL. Does tumor mutational status correlate with clinical response to imatinib? *Nat Clin Pract Oncol*. 2006;3:600–601.
- Heinrich MC, Corless CL, Demetri GD, et al. Kinase mutations and imatinib response in patients with metastatic gastrointestinal stromal tumor. *J Clin Oncol*. 2003;21:4342–4349.
- Heinrich MC, Corless CL, Duensing A, et al. PDGFRA activating mutations in gastrointestinal stromal tumors. *Science*. 2003;299:708–710.
- Heinrich M, Corless C, Blanke C, et al. Molecular correlates of imatinib resistance in gastrointestinal stromal tumors. *J Clin Oncol*. 2006;24:4764–4774.
- Hirota S, Isozaki K, Moriyama Y, et al. Gain-of-function mutations of c-kit in human gastrointestinal stromal tumors. *Science*. 1998;279:577–580.
- Hornick JL, Fletcher CD. Immunohistochemical staining for KIT (CD117) in soft tissue sarcomas is very limited in distribution. *Am J Clin Pathol*. 2002;117:188–193.
- Hornick JL, Fletcher CD. The role of KIT in the management of patients with gastrointestinal stromal tumors. *Hum Pathol*. 2007;38:679–687.
- Kindblom L, Remotti H, Aldenborg F, et al. Gastrointestinal pacemaker cell tumor (GIPACT): gastrointestinal stromal tumors show phenotypic characteristics of the interstitial cells of Cajal. *Am J Pathol*. 1998;152:1259–1269.
- Kumar S, Perlman E, Harris CA, et al. Myogenin is a specific marker for rhabdomyosarcoma: an immunohistochemical study in paraffin-embedded tissues. *Mod Pathol*. 2000;13:988–993.
- Lasota J, Vel Dobosz A, Wasag B, et al. Presence of homozygous KIT exon 11 mutations is strongly associated with malignant clinical behavior in gastrointestinal stromal tumors. *Lab Invest*. 2007;87:1029–1041.
- Liegl B, Kepten I, Le C, et al. Substantial heterogeneity of kinase inhibitor resistance mechanisms in GIST. *J Pathol*. 2008. In press.
- Pauwels P, Debiec-Rychter M, Stul M, et al. Changing phenotype of gastrointestinal stromal tumours under imatinib mesylate treatment: a potential diagnostic pitfall. *Histopathology*. 2005;47:41–47.
- Sarlomo-Rikala M, Kovatch A, Barusevicius A, et al. CD117: a sensitive marker for gastrointestinal stromal tumors that is more specific than CD34. *Mod Pathol*. 1998;728–734.
- Therasse P, Le Cesne A, Van Glabbeke M, et al. RECIST vs. WHO: prospective comparison of response criteria in an EORTC phase II clinical trial investigating ET-743 in advanced soft tissue sarcoma. *Eur J Cancer*. 2005;41:1426–1430.
- Verweij J, Casali PG, Zalcberg J, et al. Progression-free survival in gastrointestinal stromal tumors with high-dose imatinib: randomised trial. *Lancet*. 2004;364:1127–1134.
- Wardelmann E, Merkelbach-Bruse S, Pauls K, et al. Polyclonal evolution of multiple secondary KIT mutations in gastrointestinal stromal tumors under treatment with imatinib mesylate. *Clin Cancer Res*. 2006;12:1743–1749.